

was not required, and it is argued that in view of the present results this background correction must be viewed with suspicion. The parameters governing the many-body singularities derived in this way are the most accurate available to date. A quantitative interpretation of these parameters is in most cases only possible within limits because of the complexity of the band structures. Finally, in view of these results, it is hard to escape the conclusion that the MND theory must also apply in other spectroscopies which involve the generation of core holes in metals.¹¹

*Permanent address: Fachbereich Physik, Freie Universität, Berlin, Republic of West Germany.

¹G. D. Mahan, Phys. Rev. **163**, 612 (1967).

²P. Nozières and C. T. De Dominicis, Phys. Rev. **178**, 1097 (1969).

³See also K. D. Schotte and U. Schotte, Phys. Rev.

182, 479 (1969); D. C. Langreth, Phys. Rev. **182**, 973 (1969).

⁴S. Doniach and M. Sunjic, J. Phys. C: Proc. Phys. Soc., London **3**, 285 (1970).

⁵S. Hüfner and G. K. Wertheim, Phys. Rev. B **11**, 678 (1975).

⁶Other recent work has not attempted a comparison between theoretical and experimental line shapes. See, for example, S. Hüfner, G. K. Wertheim, D. N. E. Buchanan, and K. W. West, Phys. Lett. **A46**, 420 (1974); N. J. Shevchik, Phys. Rev. Lett. **33**, 1336 (1974); L. Ley, F. R. McFeely, S. P. Kowalczyk, J. G. Jenkin, and D. A. Shirley, Phys. Rev. B **11**, 600 (1975).

⁷S. Hüfner, G. K. Wertheim, and D. N. E. Buchanan, Chem. Phys. Lett. **24**, 527 (1974).

⁸S. Hüfner, G. K. Wertheim, and J. H. Wernick, to be published.

⁹A. Kotani and Y. Toyozawa, J. Phys. Soc., Jpn. **35**, 1082 1073 (1973), and **37**, 912 (1974).

¹⁰G. K. Wertheim and P. H. Citrin, unpublished.

¹¹See J. D. Dow, Phys. Rev. B **9**, 4165 (1974), for a summary of attempts to demonstrate the MND mechanism in other spectroscopies.

Chemical Bonding and Structure of Metal-Semiconductor Interfaces

J. M. Andrews

Bell Laboratories, Allentown, Pennsylvania 18103

and

J. C. Phillips

Bell Laboratories, Murray Hill, New Jersey 07974

(Received 9 April 1975)

New results and new microscopic models are presented to describe chemical trends in barrier heights at transition-metal-silicide-silicon interfaces and at nontransition-metal-silicon interfaces, where in the latter case a very thin oxide is present.

Broadly speaking there are four kinds of interfaces between metals and nonmetals. Each type is characterized by specific interfacial atomic configurations and chemical interactions. Within each type the barrier height ϕ_B for thermionic emission of electrons across the interface exhibits characteristic chemical trends.¹⁻³ The four types are as follows: (1) The nonmetal is an insulator, and the metal is physisorbed on the insulator surface. (2) The nonmetal is a highly polarizable ($\epsilon > 7$)³ semiconductor (such as Si) and the metal does not react with it to form a bulk compound (weak chemical bonding). (3) The nonmetal is a highly polarizable semiconductor and there are one or more bulk compounds which can be formed between it and the metal (strong

chemical bonding). (4) The surface preparation (e.g., by chemical etching rather than by cleaving in very high vacuum) of the highly polarizable semiconductor has left a very thin oxide between it and the metal (bonding mediated by a native dielectric).

Type (1) is a true Schottky barrier, in which ϕ_B is nearly proportional to ϕ_m , the metal work function.⁴ Type (2) is a Bardeen barrier,⁵ in which ϕ_B is nearly independent of ϕ_m . In this Letter we propose for the first time microscopic models of the potentials associated with interfaces of types (3) and (4). These models account for the chemical trends in ϕ_B observed for types (3) and (4). The chemical trend of type-(3) interfaces as reported here is new, while the trend

TABLE I. Barrier heights and heats of formation of transition-metal silicides (in their most stable stoichiometries) against n -type Si. Heats of formation are measured per tm atom, and the value for Au, which does not form a silicide, is included for fiducial purposes; the value quoted is typical for Van der Waals binding.

tmSi	ϕ_B (eV)	ΔH_f (eV)
PtSi	0.87	0.68
Au	0.79	~ 0.09
Pt ₂ Si	0.78	0.45
Pd ₂ Si	0.745	0.45
RhSi	0.69	0.70
NiSi	0.66	0.89
WSi ₂	0.65	0.97
CoSi ₂	0.65	1.07
TiSi ₂	0.60	1.40
TaSi ₂	0.59	1.21
CrSi ₂	0.57	1.26
MoSi ₂	0.55	1.36
ZrSi ₂	0.55	1.55

for type-(4) interfaces was given by Turner and Rhoderick (TR).⁶

Experimental data on type-(3) interfaces are most extensive for the transition-metal-silicide-silicon (tmSi-Si) interfaces discussed explicitly here, but the behavior of other type-(3) interfaces is expected to be similar. Type-(3) interfaces have been thoroughly studied because the formation of tmSi's by a solid-state metallurgical reaction provides the most reliable and reproducible metal-semiconductor (m-s) barriers.⁷⁻¹⁰ The reaction causes the interface to move into the interior of the silicon lattice away from surface imperfections and contamination.

We have attempted to correlate the barrier heights ϕ_B (tmSi-Si) listed^{11,12} in Table I with the work functions of the metals and with their Pauling-Gordy electronegativities.¹³ Neither correlation was satisfactory. However, the correlation with the heats of formation¹¹ ΔH_f (tmSi) is excellent, providing that ΔH_f is normalized *per tm atom per formula unit*. This correlation is shown in Fig. 1, where the linear relation is the result of a least-squares fit to the data with PtSi excluded. This special case is discussed below.

The first surprising feature of Fig 1 is that a simple linear relation holds. In Pauling's picture¹³ of strong chemical bonding the charge transfer q between the tm and Si should be proportional to $(-\Delta H_f)^{1/2}$, and in Bardeen [type-(2)]

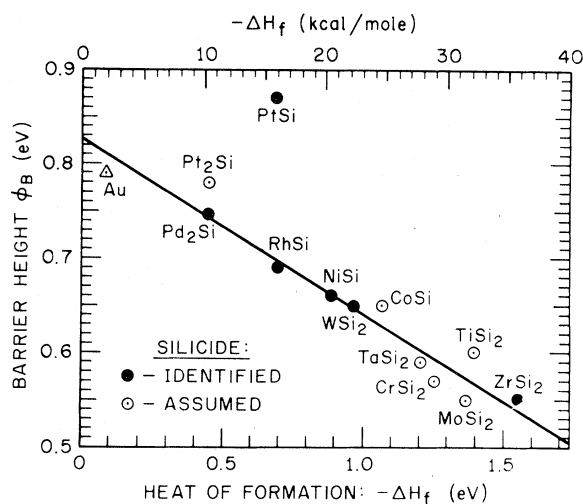


FIG. 1. Barrier heights of tmSi-Si interfaces plotted against heats of formation ΔH_f of the identified (assumed) tmSi compound. The point for Pt₂Si is discussed in the special note at the end of this paper. The correlation coefficient (excluding the PtSi datum) is 97%. $\phi_B = 0.83 + 0.18\Delta H_f$.

barriers the shift in the barrier height is proportional to q . Pauling's picture has been shown¹⁴ to account both for ΔH_f and for q [as measured independently by electron spectroscopy for chemical analysis (ESCA)] in tm carbides, nitrides, and oxides with the (substantially) ionic NaCl structure. However, tm-metalloid compounds with the metalloid (an element from columns IV, V, or VI) not belonging to the first period characteristically exhibit weakly ionic structures dominated by chains or planes of strongly bonded tm atoms, with the tm-metalloid bonding being of secondary importance.¹⁵ In such cases where the tm-Si bonds are long and the interactions are weak, it seems likely that the degree of hybridized bonding between tm and silicon atoms would be linear in $-\Delta H_f$. With increasing values of $-\Delta H_f$ more sp^3 orbitals are mixed into the tm d orbitals, and to first order the degree of admixture is proportional to $-\Delta H_f$. With sufficiently strong sp^3 admixture, the hybridized orbitals about the tm atom would become very similar to those about a Si atom and the barrier height would go to zero.

This simple argument can be used not only to justify the linearity of the fit in Fig. 1, but also to explain the slope and intercept as well. In the limit $\Delta H_f \rightarrow 0$ (e.g., Au-Si interfaces, with a very small Van der Waals binding) ϕ_B equals the free-Si-surface value¹⁶ of 0.83 eV. The intercept ϕ_B

= 0 (obtained by extrapolation) is $-\Delta H_f = 4.8$ eV per tm atom or 110 kcal/mole, which corresponds almost too well with the cohesive energy of Si (108 kcal/mole¹²). Note that in elemental tm's the charge distribution can be represented accurately by a superposition of unhybridized, spherically symmetric, charge distributions centered on each tm site. Similarly the charge distribution of free Si atoms is spherically symmetric, and the atoms are in unhybridized states. We may say that the hybridization energy needed to make tm-Si bonds indistinguishable from Si-Si bonds is practically identical to the hybridization energy of the Si bonds themselves. Thus the slope in Fig. 1 is determined by Si itself, which acts as its own fiducial point to determine the extrapolated intercept $\varphi_B = 0$.

The exception to the fit in Fig. 1 is $\varphi_B(\text{PtSi-Si})$, which also exhibits¹⁷ substantial long-range order in the interfacial plane, in contrast to most tmSi-Si interfaces, where near the interface the tmSi is probably disordered (amorphous). Electron diffraction studies show that 200-Å-thick PtSi films on (11) Si possess a strong degree of preferred orientation with grains which are triply positioned with (100) PtSi parallel to (111) Si and [010] PtSi parallel to $\langle 110 \rangle$ Si. On going to thicker films other orientations are obtained, which suggests that rearrangement can occur away from the interface because of strain energy in the PtSi film. At the interface with the apparently epitaxial configuration characteristic of 200-Å films the bonding between the final Pt layer of PtSi and the first Si layer is probably ionic covalent (rather than metallic covalent, as suggested above for other tmSi-Si interfaces), because Pt and Si atoms are arranged in layers parallel to the interface.¹⁷ Partially ionic bonding would result in electron transfer to interface states. This transfer can explain the anomalously high value of $\varphi_B(\text{PtSi-Si})$, which is 0.05 eV larger than $\varphi_B(\text{Au-Si})$.

In a classic study of type-(4) interfaces TR⁶ have shown that when the Si surface is cleaned by a variety of chemical methods, $\varphi_B^{(4)}(\text{m-Si})$ (after aging for a period of time dependent on the chemical method) reaches a final value independent of the chemical method. By contrast, type-(2) or Bardeen barriers have $\varphi_B^{(2)}(\text{m-Si}) \approx \varphi_B^{(2)}(\text{Au-Si}) = 0.8$ eV. The barrier heights satisfy the relation⁶ (here m is Pb, Al, Ag, Cu, or Au)

$$\varphi_B^{(2)}(\text{m-Si}) - \varphi_B^{(4)}(\text{m-Si}) = (\varphi_m - \varphi_0) / \epsilon_{\text{ox}}, \quad (1)$$

with $\varphi_0 = 4.7 \pm 0.2$ eV and $\epsilon_{\text{ox}} = 1.5 \pm 0.1$. The value

of $\varphi_0 = 4.7$ eV as a reference energy puzzled TR, who could only conclude that it "accidentally coincided" with φ_{Au} .

In discussing type-(3) interfaces we have seen that Si serves as its own fiducial point, and $\varphi_{\text{Si}} = 4.8$ eV.¹⁶ This suggests that the very thin oxide between m and Si is polarized by the contact potential $\varphi_m - \varphi_{\text{Si}}$, and that ϵ_{ox} is in fact nothing more than the effective dielectric constant for this oxide. The optical dielectric constant for SiO₂ is¹² $\epsilon = 2.34$, which is much larger than ϵ_{ox} . We infer, because tunneling takes place through the thinnest parts of the oxide, that at these points the oxide may consist of only one oxygen atom, for which $\epsilon_{\text{ox}} \approx 1.5$ is appropriate. (TR suggest that the oxide may be 10–20 Å thick on the average.)

The results derived here have indirect but strong implications for the nature of chemical bonding at type-(2) interfaces. These implications, which contradict pictures of bonding derived from electron diffraction and other studies of submonolayer metal-semiconductor geometries, are discussed elsewhere.¹²

After completion of this manuscript, our attention was drawn to recent studies¹⁸ of Pt:Si Schottky barriers. Barriers on Si {111}, {100}, and {110} crystal faces were prepared by sputtering Pt on Si and either annealing at 600°C or heating (to about 500°C) the Si substrate (without annealing), the latter being described as "'low temperature' PtSi-Si." Of the six possible configurations, five gave $\varphi_B \approx 0.87$ eV, in agreement with the value given in Table I. Low-temperature Pt on Si(111), however, gave $\varphi_B = 0.780 \pm 0.002$ eV (1750 samples). We explain this by assuming that (only) on the most stable Si(111) face have the usual reaction kinetics¹⁹ ($\text{Pt} + \text{Si} \rightarrow \text{Pt}_2\text{Si} \rightarrow \text{PtSi}$) been arrested near the Pt₂Si stage by the device of substrate heating during Pt deposition rather than annealing after deposition. There is no direct way to determine experimentally the chemical composition of tmSi at the interface, so that Cordes, Garfinkel, and Taft¹⁸ "do not understand how this material [low-temperature PtSi:Si(111)] is different from conventionally formed PtSi-Si contacts." However, from Fig. 1 it is apparent that they have devised a way of forming Pt₂Si-Si contacts.

We are grateful to A. K. Sinha for helpful conversations, and to M. P. Lepselter for drawing our attention to Ref. 18.

¹There are, of course, transitions between the four

types, but as these are generally abrupt, we have omitted them here. For example, the Mead transition between types (1) and (2) is described in S. Kurtin, T. C. McGill, and C. Mead, *Phys. Rev. Lett.* **22**, 1433 (1969). In J. C. Phillips, *Solid State Commun.* **12**, 861 (1973), it is shown that the type-(1) \rightarrow type-(2) transition is determined by the critical polarizability ϵ_c of the nonmetal which separates semiconductors from insulators. This critical polarizability ϵ_c is about 6-7, and the value of ϵ_c is also derived microscopically by Phillips. As noted in Kurtin, McGill, and Mead, the abruptness of the transition suggests a phase transformation, which is the basis of our classification.

²Kurtin, McGill, and Mead, Ref. 1.

³Phillips, Ref. 1.

⁴W. Schottky, *Z. Phys.* **118**, 539 (1942).

⁵J. Bardeen, *Phys. Rev.* **71**, 717 (1947).

⁶M. J. Turner and E. H. Rhoderick, *Solid State Electron.* **11**, 291 (1968).

⁷M. P. Lepselter and J. M. Andrews, in *Ohmic Contacts to Semiconductors*, edited by B. Schwartz (Electrochemical Society, Princeton, N. J., 1969), p. 159.

⁸J. M. Andrews and M. P. Lepselter, *Solid State Electron.* **13**, 1011 (1970).

⁹J. M. Andrews and F. B. Koch, *Solid State Electron.* **14**, 901 (1971).

¹⁰C. J. Kircher, *Solid State Electron.* **14**, 507 (1971).

¹¹The references for the data on ΔH_f and φ_B are collected in J. C. Phillips and J. M. Andrews, to be published.

¹²Phillips and Andrews, Ref. 11.

¹³L. Pauling, *Nature of the Chemical Bond and the Structure of Molecules and Crystals: An Introduction to Modern Structural Chemistry* (Cornell Univ. Press, Ithaca, N.Y., 1960), p. 91 ff.

¹⁴J. C. Phillips, *J. Phys. Chem. Solids* **34**, 1051 (1973).

¹⁵The chain structure of tm-metalloid compounds is discussed for the simplest cases (NiAs and MnP structures, to which the simplest silicides belong) by P. Eslinger and K. Schubert, *Z. Metallkd.* **48**, 126 (1957). See especially p. 130.

¹⁶G. W. Gobeli and F. G. Allen, *Phys. Rev.* **137**, A245 (1965).

¹⁷A. K. Sinha *et al.*, *J. Appl. Phys.* **43**, 3637 (1972).

¹⁸L. F. Cordes, M. Garfinkel, and E. A. Taft, NASA Contract Report No. 3-16749, 1974 (unpublished).

¹⁹J. M. Poate and T. C. Tisone, *Appl. Phys. Lett.* **24**, 391 (1974).

Experimental Contribution to the Summation Problem of Pinning Forces in Type-II Superconductors

G. Antesberger and H. Ullmaier

Institut für Festkörperforschung der Kernforschungsanlage, D 517 Jülich, Germany

(Received 14 April 1975)

The pinning-force density P_v in Nb single crystals containing platelike Nb₂N precipitates shows a strong dependence on the orientation of the precipitates with respect to the flux-line direction. Using purely geometrical arguments this anisotropy can be quantitatively explained by assuming that $P_v \propto K_0^2$, where K_0 is the individual flux-line-defect interaction force. This points to a summation process which is governed by the elastic behavior of the flux lattice.

In an ideal type-II superconductor the flux-line assembly in the mixed state will begin to move and to dissipate energy whenever a force acts on it. Since a transport current perpendicular to the field direction produces such a force, ideal type-II superconductors are not able to carry transport currents without losses. Technologically useful materials therefore contain extended lattice defects (pinning centers) which prevent the flux lattice from moving until the applied force density P_D exceeds a critical value. The corresponding critical current density j_c is given by the condition that P_D just equals the maximum pinning-force density P_v ("critical state")^{1,2)}

$$- \vec{P}_D = \vec{B} \times \vec{j}_c = \vec{P}_v. \quad (1)$$

The pinning-force density is a function of the flux density B , the temperature T , and the defect structure of the superconductor. Several measuring techniques have been developed which permit an accurate determination of P_v and reliable data for a vast number of different superconductors and defect structures are now available. However, it is still a point of controversy how these macroscopic results should be correlated with theoretical treatments of the different "microscopic" pinning processes,³ i.e., with the individual flux-line-defect interaction forces K . Two different views are advocated:

(A) In this approach one assumes that the strong coupling of flux lines to each other prevents them from adjusting to the array of pinning centers in